

Full Research Paper

## Noncovalently Modified Carbon Nanotubes with Carboxymethylated Chitosan: A Controllable Donor-Acceptor Nanohybrid

Dewu Long, Guozhong Wu \*, Guanglai Zhu

Department of Nuclear Analysis, Shanghai Institute of Applied Physics, Chinese Academy of Sciences, Shanghai 201800, P.R. China

\* Author to whom correspondence should be addressed. Tel./Fax: 86-21-5955 8905; E-mail: wuguozhong@sinap.ac.cn

Received: 4 January 2008 / Accepted: 31 January 2008 / Published: 5 February 2008

---

**Abstract:** We report here the modification of multiwalled carbon nanotubes (MWNTs) with a kind of polysaccharide, carboxymethylated chitosan (cmCs), and their potential usage as donor-acceptor nanohybrids. The modified composites (cmCs/MWNTs) were characterized by high-resolution TEM, FT-IR, TGA and time-resolved spectroscopy. The time-resolved spectroscopic experiments revealed that interfacial electron transfer readily takes place between MWNTs and surface immobilized cmCs chains. The forward electron transfer is fast ( $< 20$  ns) while the backward recombination is slow. The recombination process strongly depends on the chain length of carboxymethylated chitosan, i.e. a shorter recombination lifetime ( $\sim 1.1$   $\mu$ s) for the shorter-chain cmCs coated MWNTs against that of the longer-chain cmCs coated MWNTs ( $\sim 3.5$   $\mu$ s). The results demonstrated that the cmCs/MWNTs composite may be applied as a controllable donor-acceptor nanohybrid.

**Keywords:** multiwalled carbon nanotubes; carboxymethylated chitosan; charge separation; donor-acceptor nanohybrid.

---

### 1. Introduction

Carbon nanotubes (CNTs) have attracted intensive attention because of their promising application in electronic devices, catalysis and biotechnology [1,2]. However, the weakly dispersive property of

CNTs in common solvents draws back their application in many fields. Various strategies have been applied to improve their dispersion properties by immobilization of soluble organic molecules to CNTs [3-5]. Of particular interest is the modification of CNTs by photoactive molecules, such nanohybrids are regarded as donor-acceptor models and as building blocks in optoelectronic devices [6-9]. Knowledge of the charge separation process of the CNTs-based nanohybrids is helpful in understanding of the interactions between CNTs and surface molecules, enabling one to design nano-devices by the use of suitable molecules for immobilization. There were a few reports on the investigation of photoinduced interfacial electron transfer between photoactive molecules (e.g. porphyrin [6], ferrocene[7] and pyrene[8-9]) and CNTs. Photoinduced charge separation was observed for the modified ensembles and CNTs usually acted as electron acceptors in these systems. A kind of controllable nanohybrids was recently reported by Herranz and co-workers using tetrathiafulvalene as a photosensitizer [10]. They found that the charge separation could be controlled via solely changing the length of spacer chain.

Chitosan is a natural and biocompatible polysaccharide with glucosamine as the basic unit (chemical structure can be found in Figure S1). The amounts of amine and hydroxyl groups in their glucosamine units are important for some bioengineering applications [11,12]. Some researchers have reported the modification of CNTs with chitosan [13,14] or cellulose [15] via their  $\pi$ - $\pi$  stacking and hydrophobic interactions. Electrochemical measurement revealed that electrons can be hoppingly transported in chitosan coated CNTs electrode, indicating that CNTs coated with chitosan can accept and transport electrons [16-17]. As chitosan is soluble only in weak acidic solution, carboxymethylated chitosan (referred hereinafter as cmCs, chemical structure can be found in Figure S1), may be a better choice because it is soluble in aqueous solution over a wide range of pH.

We report in this paper the modification of MWNTs with cmCs, and subsequently investigation of their photoinduced electron transfer process by laser photolysis. The results indicated that photoinduced electron transfer occurs between surface immobilized cmCs and MWNTs within 20 ns for cmCs/MWNTs nanohybrids. It is found that the recombination process in nanohybrids is strongly dependent on the length of surface cmCs chain. A longer-lived transient species was observed for the longer-chain cmCs coated MWNTs nanohybrids. This long-lived intermediate was assigned to cmCs radicals due to their wrapping and folding on the surface of MWNTs. The results imply that the cmCs modified MWNTs may be used as a controllable donor-acceptor nanohybrid.

## 2. Experimental Section

### 2.1. Reagents and materials

MWNTs were purchased from Shenzhen Nanotech Port Co., Ltd., synthesized by chemical vapor deposition method (purity >95%, 20-35 nm in diameter) and used without further purification. cmCs were purchased from Zhejiang Yuhuan Biochemical Co. Ltd.; the average molecular weights of two samples determined by Gel Permeation Chromatography (GPC) were 17 000 (cmCs1) and 7 000 (cmCs2). Aqueous GPC was performed using a  $\text{CH}_3\text{CHOONa}/\text{CH}_3\text{COOH}$  (0.05M/0.05M, 0.1 M  $\text{NaNO}_3$ ) buffer solution as eluant at 35°C, using a Waters pump and a differential reflective index detector, calibrated with pullulan standard samples. Milli-Pore water was used throughout all experiments.

## 2.2. Preparation of cmCs/MWNTs nanohybrids

Typical modification procedures of MWNTs are illustrated as follows. 7.5 mg MWNTs was mixed with 2.5 mg cmCs with several drops of water and milled in agate mortar for 10 min to get exfoliative black solid. Then the solid was thoroughly washed with water and centrifugated at 12 000 rpm/min for 20 min to remove the non-immobilized cmCs. The obtained composites were then directly dispersed in water without drying, because previous reports [15,17,18] indicated that chitosan modified CNTs can be rebundled after drying via  $\pi$ - $\pi$  coupling of the immobilized molecules. In this work, cmCs1 and cmCs2 denote cmCs samples having molecular weights of 17000 and 7000, respectively, and cmCs1/MWNTs and cmCs2/MWNTs denote the MWNTs modified with cmCs1 and cmCs2, respectively.

## 2.3. Characterization of functionalized-MWNTs

UV-visible absorption spectra were obtained from Hitachi-3010 spectrophotometer. FT-IR spectra were recorded on Nicolet Avater-360 spectrometer using KBr pellets. Thermogravimetric Analysis (TGA) measurement was performed with a Perkin-Elmer Pyris-1 series thermal analysis system, at a scan rate of 10°C/min in air. High-resolution TEM was observed with a JEOL JEM-2011 at an accelerating voltage of 200 kV. The samples for TEM observations were prepared by dropping the modified-MWNTs suspension onto a carbon-coated copper grid for 30 s and then blotting off. Fluorescence measurement was performed with a Hitachi-4500 spectrofluorometer.

Details of the laser photolysis system can be found elsewhere [19]. Briefly, a Nd:YAG laser with a wavelength of 266 nm (fourth harmonic, output ~10 mJ/pulse, pulse width 3-6 ns) was used as the excitation source. A 300 W high-pressure Xenon-mercury lamp provided a continuous light for monitoring of the transient absorption spectra. The angle between pump laser and probe light was 90°. The light transmitted from the sample was monochromated and collected by a photomultiplier tube and then transferred into an oscilloscopic trace, and finally recorded by a computer.

# 3. Results and Discussion

## 3.1. Preparation and characterization of cmCs/MWNTs nanohybrids

Unlike the pristine MWNTs, cmCs/MWNTs can easily disperse in water to form a black solution (Figure S2). These solutions can be stably stored at ambient temperature for several months. The presence of cmCs on the surface of MWNTs was characterized by means of UV-vis and FT-IR spectra. Figure 1A shows the UV-vis absorption spectra of the modified MWNTs and also the spectrum of cmCs alone. The absorption spectra of cmCs1/MWNTs and cmCs2/MWNTs show broad signals monotonically decreasing from 200 to 800 nm as previously reported for MWNTs [6], indicating the presence of MWNTs in this solution. An additional featureless peak at 250-380 nm was observed for the modified-MWNTs, corresponding to the characteristic absorption of glucosamine unit of cmCs. FT-IR spectra (Figure 1B) of cmCs/MWNTs clearly show typical N-H scissoring vibrations of glucosamine at 1650  $\text{cm}^{-1}$  (amide I) and symmetric stretch of C-O-C at 1020-1075  $\text{cm}^{-1}$  [20,21].

Strong peaks due to O-H vibrations at  $3300\text{ cm}^{-1}$  were also clearly observed for the modified MWNTs. These results confirm the noncovalent immobilization of cmCs chains onto MWNTs.

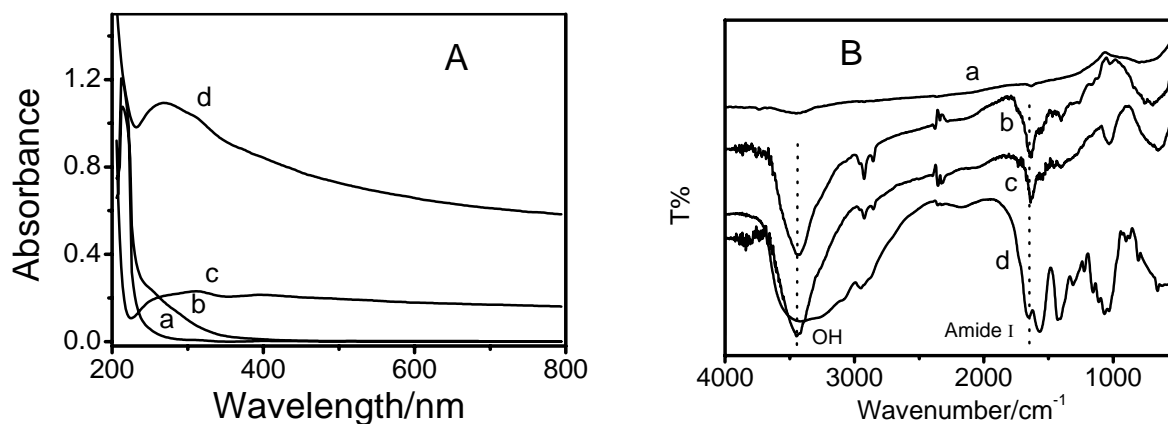


**Figure 1.** **A:** UV-Vis spectra of (a) cmCs1, (b) cmCs2, (c) cmCs1/MWNTs and (d) cmCs2/MWNTs, respectively; and **B:** FT-IR spectra of (a)pristine MWNTs, (b) cmCs1/MWNTs, (c) cmCs2/MWNTs, and (d) cmCs, respectively.

Further evidence indicating the presence of cmCs at the MWNT surface was obtained by HRTEM. As shown in Figure 2, a uniform amorphous coated cmCs layer is clearly identified. Moreover, thickness of the polymer layer on the MWNT surface varies with the molecular weight of cmCs. Higher molecular weight leads to a thicker surface layer, i.e. 3 nm for cmCs1/MWNTs and 1-2 nm for cmCs2/MWNTs. This difference in thickness is due to the wrapping and folding of longer polysaccharide chains via  $\pi$ - $\pi$  stacking on the MWNT surface [13,21].

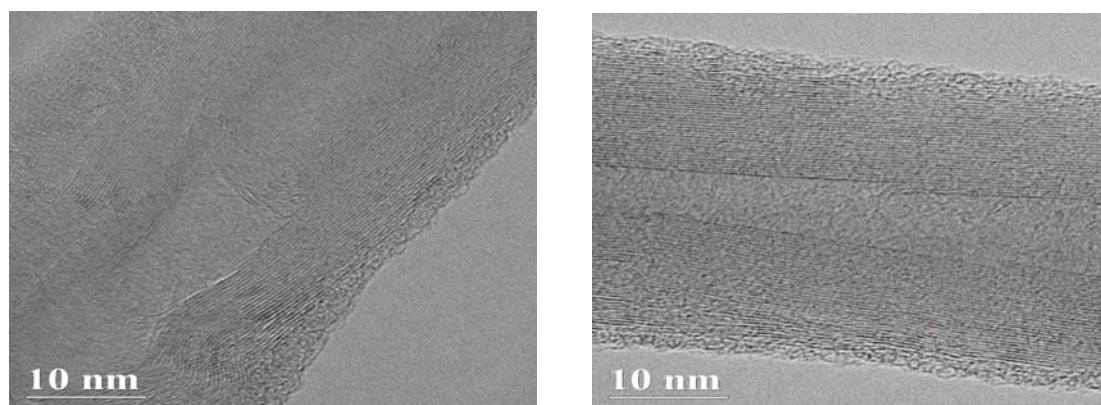


**Figure 2.** HRTEM observations of cmCs1/MWNTs (Left) and cmCs2/MWNTs (Right).

Figure 3 shows TGA curves of the modified-MWNTs, pristine MWNTs, and cmCs. The weight loss of pristine MWNTs starts at  $400\text{ }^{\circ}\text{C}$  and a significant loss is observed at  $600\text{--}800\text{ }^{\circ}\text{C}$ , indicating the decomposition of MWNTs at high temperature. It is noted that about 20% weight of the pristine MWNTs is remained even at  $>800\text{ }^{\circ}\text{C}$ . This is probably due to the presence of transition metals introduced in the synthesis, in accordance with the literature report [17]. The TGA curves of cmCs1/MWNTs and cmCs2/MWNTs both exhibit two weight loss regions at  $<100\text{ }^{\circ}\text{C}$  and  $250\text{--}350\text{ }^{\circ}\text{C}$ ,

while the major weight loss is at 400-800°C. The weight loss at 400-800°C can be ascribed to the decomposition of MWNTs, while the weight loss below 400°C is due to the decomposition of the cmCs layers immobilized on the MWNTs. The weight loss at <100 °C is assigned to the detachment of water contained in the cmCs chains, since water molecules can be trapped in the cmCs crystal via hydrogen bonding [17]. The weight loss at 250-350°C is due to the thermal decomposition of backbone chains of cmCs [17,24,25]. The percentages of cmCs coated on the MWNTs determined from the TGA measurement were 17.6 wt% and 11.4 wt% for cmCs1/MWNTs and cmCs2/MWNTs, respectively( see the ESI for details of calculation). This result is in agreement with the observed different thicknesses of polymer layers by HRTEM.

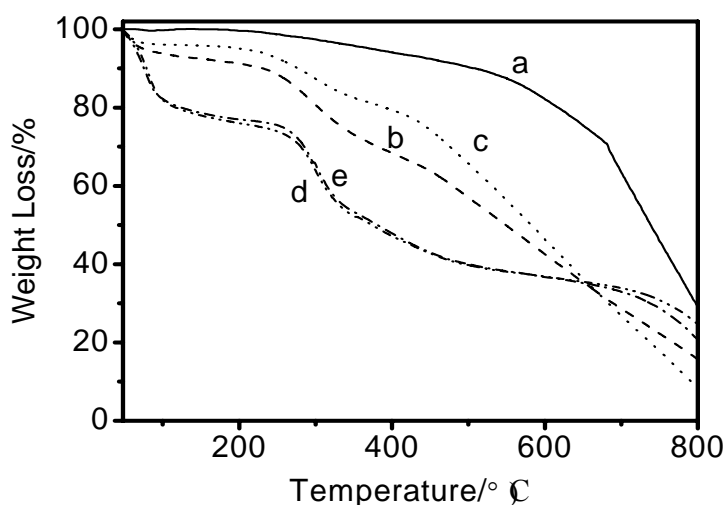


**Figure 3.** TGA curves of (a) pristine MWNTs, (b) cmCs1/MWNTs, (c) cmCs2/MWNTs, (d) cmCs1 and (d) cmCs2 in air.

### 3.2. Photoinduced charge separation of cmCs/MWNTs nanohybrids

As shown in Figure 4, an intensive emission peak centered at 430 nm is observed for cmCs aqueous solution upon excitation at 320 nm. To the contrary, no discernible emission peak is observed when cmCs is attached to the surface of MWNTs. The emission quenching implies a strong interaction between the surface immobilized cmCs and MWNTs. This emission quenching results from either electron transfer or energy transfer between surface bound cmCs and MWNTs. Similar emission quenching was also observed using excitation wavelength of 350 nm, indicating the occurrence of electron transfer between cmCs and MWNTs. Moreover, addition of cmCs into this solution caused gradually an increase of the emission intensity, ruling out the intermolecular interaction between free cmCs molecules and MWNTs.

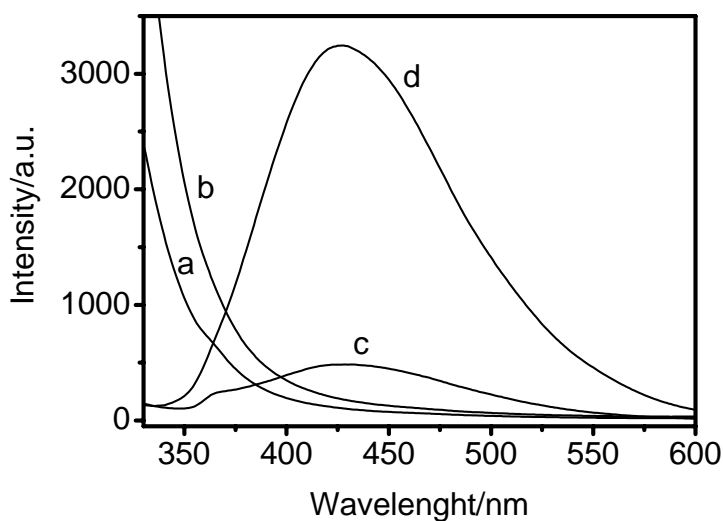


**Figure 4.** Fluorescence spectra of (a) cmCs1/MWNTs, (b) cmCs2/MWNTs, (c) cmCs1 and (d) cmCs2 after 320 nm excitation. All samples were adjusted to have the same absorption at 320 nm.

Direct evidence of photoinduced charge separation between surface immobilized cmCs and MWNTs is observed by laser photolysis. Figure 5 shows transient absorption spectra of cmCs1/MWNTs and cmCs2/MWNTs after 266 nm laser excitation as well as the transient absorption spectra for the corresponding cmCs aqueous solution. The transient absorption spectra of cmCs is mainly contributed to cmCs radicals ( $\text{cmCs}^+_{\text{aq}}$ ,  $\lambda_{\text{max}}$ : 320 nm) and hydrated electrons ( $e_{\text{aq}}^-$ ,  $\lambda_{\text{max}}$ : 720 nm) due to their photoionization by UV laser excitation. This result is in agreement with similar previous reports [22-23].

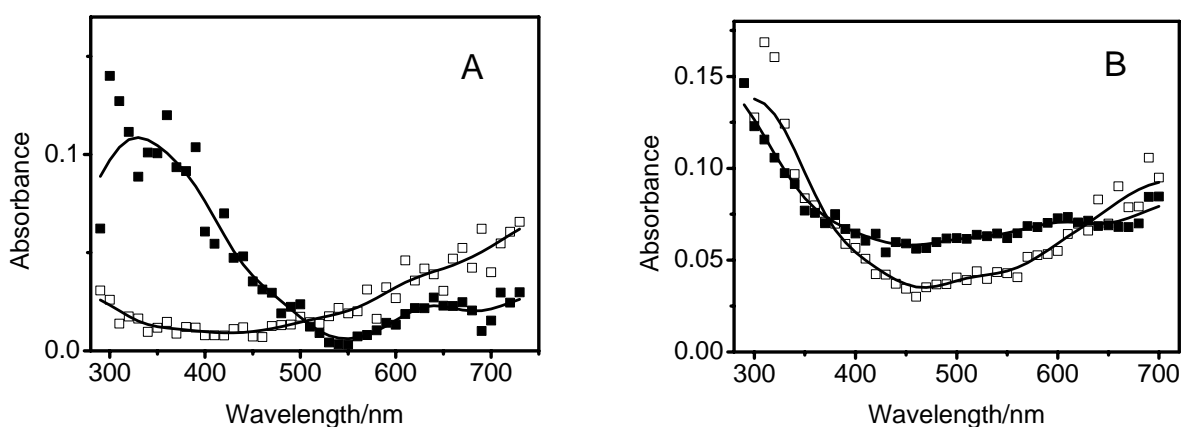


**Figure 5.** Transient absorption spectra recorded at 100 ns after 266 nm laser excitation for (A)  $\text{cmCs1}^+_{\text{aq}}$  ( $\square$ ) and  $\text{cmCs1}^+/\text{MWNTs}$  ( $\blacksquare$ ) and (B)  $\text{cmCs2}^+_{\text{aq}}$  ( $\square$ ) and  $\text{cmCs2}^+/\text{MWNTs}$  ( $\blacksquare$ ). All samples were adjusted to have the same absorption at 266 nm. The solid lines are computer fitting curves.

The transient absorption spectra of cmCs1/MWNTs and cmCs2/MWNTs, are quite different from that of free cmCs. The absorption band due to hydrated electron almost disappears while a featureless broad band is observed at 500-650 nm. The disappearance of absorption band of hydrated electron indicates the efficient scavenging of electrons by the presence of MWNTs. Therefore, the featureless absorption band at 500-650 nm may be assigned to the formation of reduced MWNT species via interfacial electron transfer from surface attached cmCs [8-9]. Another intensive transient absorption band is observed in the UV regions in Fig.5, both for cmCs1/MWNTs and cmCs2/MWNTs. This transient species is assigned to the radical of chitosan at the surface of MWNTs (cmCs<sup>+</sup>/MWNTs), in accordance with the previous reports [22-23]. The formation of cmCs radical and the reduced MWNTs species in the nanohybrids is an evidence indicating the interfacial electron transfer between immobilized cmCs and MWNTs.

The recombination of cmCs radicals and the shuttle electrons in the modified nanohybrids (cmCs<sup>+</sup>/MWNTs<sup>-</sup>) can be monitored by the decay profile of the cmCs radicals. Figure 6 shows the decay profiles of cmCs radicals at 320 nm for cmCs<sup>+</sup>/MWNTs and cmCs<sup>+</sup><sub>aq</sub>, respectively. As previously reported [22,23], the decay of free radical in solution is predominantly via the recombination of hydrated electron and radical pairs, which is a diffusion-controlled reaction. In this study, the decay profiles of cmCs radicals (cmCs<sup>+</sup><sub>aq</sub>) exhibit first-order kinetics with lifetimes of 12.0 μs for cmCs1<sup>+</sup><sub>aq</sub> and 5.8 μs for cmCs2<sup>+</sup><sub>aq</sub>.

Also shown in Figure 6 are the decay profiles of cmCs radicals at the surface of MWNTs (cmCs1<sup>+</sup>/MWNTs and cmCs2<sup>+</sup>/MWNTs), both of them exhibit different decay behavior from the free radicals in solution. The decay of cmCs2<sup>+</sup> on the surface of MWNTs is fast, with a lifetime less than 20 ns. Since this time scale is approximate to the time resolution of our apparatus, the actual process may be faster. This fast decay accounts for ~95% of the observed transient absorption, it is suggested to be the recombination of surface immobilized radicals and the shuttle electrons in MWNTs. Comparing to the lifetime of cmCs2<sup>+</sup><sub>aq</sub>, the decay of cmCs2<sup>+</sup> on the surface of MWNTs is much faster. In cmCs/MWNTs composites, the cmCs radicals are bound at the surface of MWNTs, the recombination of radical and shuttle electron on MWNTs is equivalent to intramolecular reaction and thus causes much faster decay of the cmCs radicals. Therefore, a fast decay process of surface immobilized radicals and localized electron in MWNTs were observed. The remained minor decay component (5%) is contributed by a relative longer-lived species with lifetime of 1.1 μs. It may be ascribed to the hopping transfer of electron in MWNTs [26], leading to the delocalization of electron and retarding the recombination of radicals and shuttle electrons. Similar long-lived charge separated state is also observed in porphyrin-peptide oligomers/nanotube composites [14].

In the case of cmCs1/MWNTs, the fast decay component (20 ns) immediately after pulsed laser is also clearly observed, which is assigned to a rapid recombination of radicals and shuttle electrons as formerly discussed. This absorption accounts for 80% of total observed transient absorption, as shown in Figure 6A. On the other hand, about 20% of the transient species with a lifetime of 3.5 μs is recorded in cmCs1<sup>+</sup>/MWNTs. This lifetime is significantly shorter than that of free radicals in solution (12.0 μs for cmCs1<sup>+</sup><sub>aq</sub>) but starkly longer than the rapid recombination process, and their kinetics are independent of the laser intensity on the variant of 10, 15, 20 mJ/pulse (data not be shown). This implies that this species is a new state of radicals in the nanohybrids. Due to their long molecular chain of cmCs1, therefore, the long-lived intermediates may be assigned to cmCs radicals that presented in

the long chain at the surface of MWNTs. Their lifetimes are significantly increased because of the wrapping and folding of long chains of cmCs1 on the surface of MWNTs [11]. The folded chitosan chain may significantly retard the reaction of electron-radical pairs. As reported previously [23], the reaction between chitosan and hydroxyl radical is significantly retarded when chitosan chain is coiled at lower pH solution. Therefore, the chain length-dependent recombination process implies that the backward electron transfer process can be controlled by changing the chain length of the surface-immobilized polymer, which may find use in many applications.

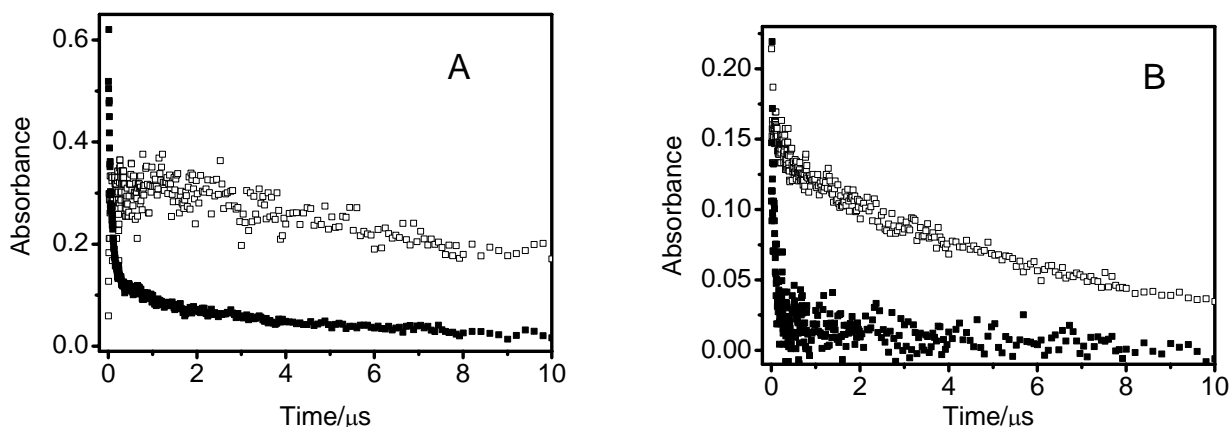


**Figure 6.** Decay profiles at 320 nm for (A) cmCs1<sup>+</sup><sub>aq</sub> (□) and cmCs1<sup>+</sup>/MWNTs (■) and (B) cmCs2<sup>+</sup><sub>aq</sub> (□) and cmCs2<sup>+</sup>/MWNTs (■). All samples were adjusted to have the same absorption at 266 nm.

#### 4. Conclusion

Noncovalently modification of MWNTs was achieved by mulling MWNTs with carboxymethylated chitosan in mortar. Laser photolysis experiment on the cmCs/MWNTs aqueous dispersion revealed that electron transfer is accessible between the surface coated cmCs molecules and MWNTs; and the charge separation process can be mediated by varying the chain length of surface coated cmCs. These cmCs modified MWNTs nanohybrids exhibit excellent controllable charge separation process, which may be useful in some special applications, such as nano-device, light conversion device and solar cells.

#### Acknowledgements

This work was jointly supported by Chinese Natural Science Foundation (Grant NO. 20573130, 20673136) and Frontier Sciences Foundation of Chinese Academy of Sciences (Grant NO. 55120703).

#### References

1. Hirsch A. Functionalization of Single-Walled Carbon Nanotubes *Angew. Chem. Int. Ed.* **2002**, *41*, 1853-1859.
2. Tasis D.; Tagmatarchis N.; Bianco A.; Prato M. Chemistry of Carbon Nanotubes *Chem. Rev.* **2006**, *106*, 1105-1136.

3. Kim Y. ; Hong S.; Jung S.; Strano M. S.; Choi J.; Baik S. Dielectrophoresis of Surface Conductance Modulated Single-Walled Carbon Nanotubes Using Catanionic Surfactants *J. Phys. Chem. B* **2006**, *110*, 1541-1545.
4. Star A.; Stoddart J. F.; Steuerman D.; Diehl M.; Boukai A.; Wong E. W.; Yang X.; Chung S. W.; Choi H.; Heath J. R. Preparation and Properties of Polymer-Wrapped Single-Walled Carbon Nanotubes *Angew. Chem. Int. Ed.* **2001**, *40*, 1721-1725.
5. Pantarotto D.; Singh R.; McCarthy D.; Erhardt M.; Briand J. P.; Prato M.; Kostarelos K.; Bianco A. Functionalized Carbon Nanotubes for Plasmid DNA Gene Delivery *Angew. Chem. Int. Ed.* **2004**, *43*, 5242-5246.
6. Baskaran D.; Mays J. W.; Zhang X. P.; Bratcher M. S. Carbon Nanotubes with Covalently Linked Porphyrin Antennae: Photoinduced Electron Transfer *J. Am. Chem. Soc.* **2005**, *127*, 6916-6917.
7. Guldi D. M.; Marcaccio M.; Paolucci D.; Paolucci F.; Tagmatarchis N.; Tasis D.; Vázquez E.; Prato M. Single-Wall Carbon Nanotube–Ferrocene Nanohybrids: Observing Intramolecular Electron Transfer in Functionalized SWNTs *Angew. Chem. Int. Ed.* **2003**, *42*, 4206-4209.
8. Martin R. B.; Qu L.; Lin Y.; Harruff B. A.; Bunker C. E.; Gord J. R.; Allard L. F.; Sun Y.P. Functionalized Carbon Nanotubes with Tethered Pyrenes: Synthesis and Photophysical Properties *J. Phys. Chem. B* **2004**, *108*, 11447-11453.
9. Ehli C.; Rahman G. M. A.; Jux N.; Balbinot D.; Guldi D. M.; Paolucci F.; Marcaccio M.; Paolucci D.; Melle-Franco M.; Zerbetto F.; Campidelli S.; Prato M. Interactions in Single Wall Carbon Nanotubes/Pyrene/Porphyrin Nanohybrids *J. Am. Chem. Soc.* **2006**, *128*, 11222-11231.
10. Herranz M.; Martin N.; Campidelli S.; Prato M.; Brehm G.; Guldi D. M.; Control over Electron Transfer in Tetrathiafulvalene-Modified Single-Walled Carbon Nanotubes *Angew. Chem. Int. Ed.* **2006**, *45*, 4478-4482.
11. Bertholon I.; Hommel H.; Labarre D.; Vauthier C. Properties of Polysaccharides Grafted on Nanoparticles Investigated by EPR *Langmuir* **2006**, *22*, 5485-5490.
12. Chen T.; Small D. A.; Wu L.; Rubloff G. W.; Ghodssi R.; R. Vazquez-Duhalt; Bentley W. E.; Payne G. F. Nature-Inspired Creation of Protein-Polysaccharide Conjugate and Its Subsequent Assembly onto a Patterned Surface *Langmuir* **2003**, *19*, 9382-9386.
13. Yang H.; Wang S. C.; Merciera P.; Akins D. L. Diameter-selective dispersion of single-walled carbon nanotubes using a water-soluble, biocompatible polymer *Chem. Commun.* **2006**, 1425-1427.
14. Saito K.; Troiani V.; Qiu H.; Solladie N.; Sakata T.; Mori H.; Ohama M.; Fukuzumi S. Nondestructive Formation of Supramolecular Nanohybrids of Single-Walled Carbon Nanotubes with Flexible Porphyrinic Polypeptides, *J. Phys. Chem. C* **2007**, *111*, 1194-1199.
15. Liu Y.; Gao L.; Sun J. Noncovalent Functionalization of Carbon Nanotubes with Sodium Lignosulfonate and Subsequent Quantum Dot Decoration *J. Phys. Chem. C* **2007**, *111*, 1223-1229.
16. Zhang M.; Gorski W. Electrochemical Sensing Platform Based on the Carbon Nanotubes/Redox Mediators-Biopolymer System *J. Am. Chem. Soc.* **2005**, *127*, 2058-2059.
17. Zhang M.; Smith A.; Gorski W. Carbon Nanotube-Chitosan System for Electrochemical Sensing Based on Dehydrogenase Enzymes *Anal. Chem.* **2004**, *76*, 5045-5050.
18. Hu C.; Chen Z.; Shen A.; Shen X.; Li J.; Hu S. Water-soluble single-walled carbon nanotubes via noncovalent functionalization by a rigid, planar and conjugated diazo dye *Carbon* **2006**, *44*, 428-434.

19. Long D.; Wu G.; Chen D.; Yao S. Spectroscopic Study the Interaction between Methyl Viologen and core-shell structure Polymer nanoparticles *Res. Chem. Intermediat.* **2005**, *31*, 613-623.
20. Tanima B.; Susmita M.; Ajay K. S.; Rakesh K. S.; Amarnath M. Preparation, characterization and biodistribution of ultrafine chitosan nanoparticles *Int. J. Pharm.* **2002**, *243*, 93-105.
21. Masatoshi S.; Minoru M.; Hitoshi S.; Hiroyuki S.; Yoshihiro S. Preparation and characterization of water-soluble chitin and chitosan derivatives *Carbohydr. Polym.* **1998**, *36*, 49-59.
22. Zhai M.; Kudoh H.; Wu G.; Wach R. A.; Muroya Y.; Katsumura Y.; Nagasawa N.; Zhao L.; Yoshii F. Laser Photolysis of Carboxymethylated Chitin Derivatives in Aqueous Solution. Part 1. Formation of Hydrated Electron and a Long-Lived Radica *Biomacromolecules* **2004**, *5*, 453-457.
23. Zhai M.; Kudoh H.; Wu G.; Wach R. A.; Muroya Y.; Katsumura Y.; Nagasawa N.; Zhao L.; Yoshii F. Laser Photolysis of Carboxymethylated Chitin Derivatives in Aqueous Solution. Part 2. Reaction of OH $\cdot$  and SO $_4^{\cdot-}$  Radicals with Carboxymethylated Chitin Derivatives *Biomacromolecules* **2004**, *5*, 458-462.
24. Sankararamakrishnan N.; Sanghi R. Preparation and characterization of a novel xanthated chitosan *Carbohydr. Polym.* **2006**, *66*, 160-167.
25. Ding W.; Q. Lian; Samuels R.J.; Polk M.B. Synthesis and characterization of a novel derivative of chitosan *Polymer* **2003**, *44*, 547-556.
26. Wang X.; Liu Y.; Yu G.; Xu C.; Zhang J.; Zhu D. Anisotropic Electrical Transport Properties of Aligned Carbon Nanotube Films *J. Phys. Chem. B* **2001**, *105*, 9422-9425.

## Appendix

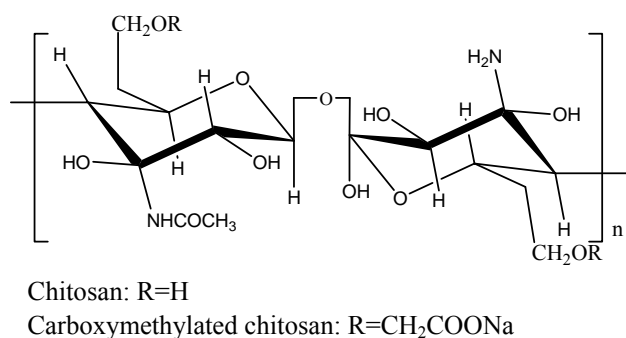


**Figure S1.** Chemical structures of chitosan and carboxymethylated chitosan



**Figure S2.** Photograph of aqueous solution of **cmCs1/MWNTs** (left) and **cmCs2/MWNTs** (right). The solutions were obtained by direct dispersion of the obtained **cmCs1/MWNTs** and **cmCs2/MWNTs** in water with vigorous shaking and then stored for a week.

*Calculation of the percentages in cmCs/MWNTs composites:*

Due to the weight loss step of surface wrapped chitosan chain in TGA is overlap with the loss of carbon nanotubes, we used the first step of the loss of complexed water in the chitosan crystal to calculate the percentages of wrapped chitosan in the composites. As to do this, a first premise is that the chitosan chains have identified affinity to water molecules either in the absence or the presence of carbon nanotube. Therefore, one can deduce the percentages of chitosan of the cmCs/MWNTs composites by following equation:  $P=L_s/L_0$ . Where P is the percentages of the chitosan in cmCs/MWNTs composites;  $L_s$  is the first loss percent < 120 °C in TGA curves of cmCs/MWNTs composites;  $L_0$  is the first loss percent < 120 °C in TGA curves of cmCs alone.